Chapter 4

Wave modelling

4.1 The wave energy balance equation

In wave modelling theoretical and observational knowledge on ocean surface waves are combined and expressed highly mathematical. The purpose of the model is to be a practical tool able to simulate the wave condition just by knowing a few easy measurable quantities. Since wind is the primary force driving waves, most models only require surface winds to operate. However, as wave models become increasingly perfected more input parameters may be necessary to maintain progress, e.g. air-sea temperature.

The wave spectrum is the most common way of describing the wave condition at a ceratin location. In modelling its evolution in time and space is often calculated using the wave energy balance equation, expressed by

$$\frac{\partial E}{\partial t} + \nabla \cdot (c_g E) = S_{in} + S_{nl} + S_{ds} \tag{4.1}$$

Eq. 4.1 is only valid in deep water. Other mechanisms also affecting the wave spectrum, like shoaling effects and currents, are not considered here.

The left hand side of eq. 4.1 constitute a local term and an advective term moving at the group velocity, c_g. The evolution of the spectrum is depending on three source functions, wind input(S_{in}), nonlinear interaction(S_{nl}) and dissipation(S_{ds}). There are continuous work being done to optimize the source function parameterizations. However, today still a lot of physical aspects concerning ocean waves are not fully understood. Empirical studies have only given us parts of the picture. In the following section the source functions are briefly discussed, with primarily focus on their influence on the wave spectrum.

4.1.1 Wind input

On short timescales wind is the only significant source of energy input to the ocean surface apart from landslides and earthquakes below the surface. The transfer of mo-

mentum between the atmosphere and ocean is a function of stress between the two media. This process is seemingly affected by several mechanisms and will be presented more in depth in chapter 5.

Quite a few studies on wind wave growth have been presented over the years, where the works by Phillips (1957);Miles (1957) stick out as the milestones. Even though the theory proposed by Miles (1957) is generally thought to give an underestimated wave growth, it still constitutes a foundation for most studies on this topic today. Several scientists have developed modified versions of Miles' theory. However, these will not be presented here. Instead a coarse description of how the wind input, S_{in}, affects the appearance of the wave spectrum is given.

Fig. 4.1 illustrates how the three source terms vary with frequency in two duration limited cases, after 3 and 96 hours respectively (Komen et al. 1996). The wind input source function is represented by connected open circles and is as expected always positive. The peak of the source term corresponds to the peak of the wave spectrum, not shown in fig. 4.1, and is similar to its overall shape, besides being less energetic. Notice how the wind input decreases with wave age, being almost divided in half comparing 3 and 96 hours duration.

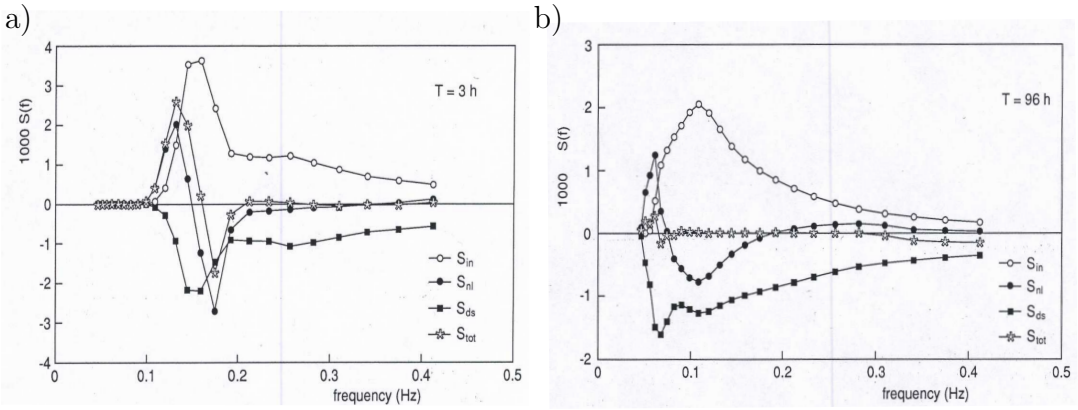

Figure 4.1: *Simulated source functions S_{in}, S_{ds} and S_{nl} for two duration limited cases obtained by the WAM-model. a) 3 hours and b) 96 hours. Figures are taken from Komen et al.(1996)*

4.1.2 Nonlinear interaction

The evolution of wind generated waves can to a certain degree of accuracy be expressed by linear theory which is possible because waves on average are not very steep. Once the steepness of the wave field increases, as is the case for wind-sea, the nonlinear processes grow more important to the evolution of the wave spectrum. The effect of nonlinear interaction is transference of energy between wave components of different frequencies. This redistribution of energy occur when interacting wave components are

in resonance. The process is conservative, not affecting the total amount of energy of the wave spectrum.

The S_{nl} is perhaps the most debated source function in the energy balance equation. The pioneering work by Hasselmann (1962) established a theoretical framework for the problem. His four-wave interaction model is a very complex and time consuming integral not to be discussed here.

The nonlinear term is characterized by a three lobe structure of opposite signs. In general, energy is being transported from frequencies around the peak of the spectrum towards higher and lower frequencies of the spectrum, with the majority going towards the latter. The nonlinear term is represented by connected black dots in fig. 4.1. For young seas, see fig. 4.1a), the positive lobe at low frequencies are centered slightly to the left of the peak frequency. This creates the *downshift* of the spectrum observed in developing seas. In the case of old seas the same positive lobe is centered closer to the peak frequency, giving a much weaker downshift. The positive lobe at the higher frequencies is smaller, but has a stronger directional distribution, giving rise to a broadening of the spectrum.

4.1.3 Dissipation

Dissipation is the least understood aspect of wind generated waves. Loss of energy in the wave field can be due to several mechanisms, like the interaction of waves with the bottom in terms of friction and wave breaking (shoaling), internal processes by viscosity and in the surface by white capping. Here, the emphasize will be on deep water where bottom interaction is negligible. The drain of energy by viscose processes are well known, but only important for wave lengths in the capillary region. The main energy loss in deep water is due to wave breaking, also known as white capping. White capping is a strong nonlinear process hard to formulate mathematically. It is highly irregular, where the actual threshold for breaking is not well understood(Massel 1996). As with the two prior source functions, only the main effect of dissipation by white capping will be presented.

Not surprisingly, also this mechanism changes with wave age. Fig. 4.1a) illustrates how the dissipation source function is more or less the mirror of the wind input after 3 hours, only slightly weaker. For an old sea, fig. 4.1b), the effect is reduced, however not as much as the wind input. Because the sea state is getting closer to its saturated state, the wind input and dissipation is almost in balance.

The sum of the three source functions are illustrated by connected stars in fig. 4.1. Notice the change in magnitude of the two functions. This is a logical behavior considering the difference in wind speed and phase speed of the dominating wave components are getting smaller with wave age.

4.2 A historical perspective on wave modelling

The need for reliable wave prediction models have become increasingly important in modern society. It is essential that the likes of oil and shipping industry receive accurate wave forecasts to operate in a safe and efficient manner. More than half a century ago the first numerical wave model was established by Gelci et al. (1957). Since then numerical modelling has come a long way. Not only do we understand the physical aspects of ocean surface waves better, now we have computer power able to calculate vast quantities of mathematical equations in a short matter of time. Still all numerical wave prediction models are based on the strive to solve the wave energy balance equation with its corresponding source terms. In the lights of this we have seen the rise of a first, second and today's third generation models.

What mainly separates the three generations of wave models are the different ways the source functions are parameterized. Especially the nonlinear term has been a huge topic of discussion. At the time Gelci et al. (1957) developed their first model the physical understanding of wind generated waves was vague, and reflected in the quality of the model. However, around the same time the important works of Phillips (1957), Miles (1957) and Hasselmann (1962) were published. These studies set the framework for future wave modelling. As a consequence, a number of new models saw the daylight in the 60s and 70s (Massel 1996).

In general, the first generation wave models did not consider any energy transference between wave components. Nonlinearities were simply ignored, $S_{nl} = 0$, or modelled in a way that had little effect on the total energy balance. Atmospheric input by wind, S_{in}, was expressed linearly and generally overestimating the energy transference. Dissipation was modelled by establishing a limiting form of the wave spectrum where the waves suddenly stopped growing. A f^{-5} saturation range was prescribed by Phillips (1958).

After extensive field and laboratory work during the 70s doubt spread about the quality of the first generation wave models. Scientists grew aware of the neglected effect of nonlinearities, as the forward face of the simulated spectrum simply grew to slow in developing seas. An attempt was also made to simulate the observed *overshoot* phenomenon of the wave spectra. In the light of this new understanding a new type of models were established. In general, we distinguish between three types of second generation models, the *discrete spectral models*(DS), the *parametric models*(P) and the combined *hybrid models*(H).

In the DS-models the wave spectrum is represented by discrete directional-frequency bins at times $t_0 + n\Delta t$ at each grid point. The energy balance equation is then solved numerically within the model area. The SWAMP-group (1985) reviewed three different types of DS-models in which all use a linear wind input function in accordance to the measurements of Snyder et al. (1981). They are limited in their growth by some form of saturation spectrum depending on the stage of development. In most models the

JONSWAP and PM spectra are used. What mainly separates these models are the way the nonlinear source function is treated. One way of solving this problem is by involving the S_{nl} implicitly in the S_{in} and S_{dis}, or by giving a coarse parametrization of the nonlinear term. The main drawback of the DS-model is the amount of calculations needed for its execution, which is drastically reduced in the P-models.

The P-models are based on the idea that as long as the nonlinear term is recognized as a controlling process, there are no need to express the other source functions in any more detail. Since the models at the time did not calculate the nonlinear source function exactly, the S_{in} and S_{dis} did not need to be expressed more precisely. Hasselmann et al. (1976) developed the first P-model. Unlike the DS-model, the wave condition and its evolution was characterized using only a few parameters. Unfortunately, the P-models only apply to developing waves and is not valid for waves outside the generating area. In other words, swell must get special attention. This is solved by combining a DS-model with a P-model, recognized as a H-model. The P-model controls the developing sea and the DS-model simulates the swell.

4.3 A third generation wave model: WAM(cycle-4)

The SWAMP-group (1985) concluded that all second generation models suffered from limitations in the nonlinear source function parametrization. Generally they performed satisfactory in fetch and duration limited cases, but showed weaknesses in extreme events with strongly varying wind fields, e.g. hurricanes, where accurate wave prediction is of special importance. By the mid-1980s numerical improvements (Hasselmann and Hasselmann (1985); Snyder et al. (1993)) made it possible to calculate the Boltzmann-type integral, the nonlinear source function, explicitly. This set the framework for the WAM(WAve-Model)-model which is described in great detail in Komen et al. (1996). In the following a brief introduction of the kinematics, source function parameterizations and numerical schemes used in the model are presented.

4.3.1 Kinematics and parametrization in the energy balance equation

The WAM-model is of the DS-type and was first implemented in 1988. It calculates the action density spectrum instead of using the variance density spectrum, defined by

$$N(f,\theta) = \frac{E(f,\theta)}{f} \tag{4.2}$$

Depending on the model area, suitable grid coordinates are chosen. In the case of a global model, the 2D spectrum is a function of angular frequency, propagation direction, latitude, longitude and time, $N(\omega, \Theta, \phi, \lambda, t)$. The energy balance equation is expressed

as follows

$$\frac{\partial N}{\partial t} + (cos\phi)^{-1}\frac{\partial}{\partial \phi}(\dot{\phi} cos\phi N) + \frac{\partial}{\partial \lambda}(\dot{\lambda} N) + \frac{\partial}{\partial \omega}(\dot{\omega} N) + \frac{\partial}{\partial \theta}(\dot{\theta} N) = S \tag{4.3}$$

in which

$$\dot{\phi} = \frac{d\phi}{dt} = (c_g cos\theta + \mathbf{U}|_{north})R^{-1} \tag{4.4}$$

$$\dot{\lambda} = \frac{d\lambda}{dt} = (c_g sin\theta + \mathbf{U}|_{east})(Rcos\phi)^{-1} \tag{4.5}$$

$$\dot{\theta} = \frac{d\theta}{dt} = c_g sin\theta tan\phi R^{-1} + \dot{\theta}_D \tag{4.6}$$

$$\dot{\omega} = \frac{\partial \Omega}{\partial t} \tag{4.7}$$

and

$$\dot{\theta}_D = \left(sin\theta \frac{\partial}{\partial \phi}\Omega - \frac{cos\theta}{cos\phi}\frac{\partial}{\partial \lambda}\Omega \right)(kR)^{-1} \tag{4.8}$$

where c_g is the group velocity, R the radius of the earth, $\Omega = \sigma + \mathbf{k} \cdot \mathbf{U}$ the dispersion relation accounting for any mean currents and S the sum of the source functions;

$$S = S_{in} + S_{nl} + S_{dis} + S_{bot} \tag{4.9}$$

Today the physical knowledge on S_{in} and S_{nl} are both of such complexity, that both terms need considerably computer power to be exactly calculated. It is therefore necessary to parameterize these two source functions into more time efficient expressions.

The wind input term is based on the theory proposed by Miles (1957). By always assuming a logarithmic wind profile, he concluded the growth rate of wind generated waves only to depend on two parameters

$$x = \frac{u_*}{c} cos(\theta - \phi) \quad \text{and} \quad \Omega_m = \kappa^2 \frac{g z_0}{u_*^2} \tag{4.10}$$

where $\kappa = 0.4$ is the von Kármán constant, c the phase speed of the waves, θ the direction in which the waves propagate and ϕ the wind direction. Ω_m is known as the profile parameter. These two parameters depends on the roughness of the airflow above the surface and is therefore dependent on the sea state. The WAM-model uses a growth rate, γ, defined by Janssen (1991) expressed as

$$\frac{\gamma}{\omega} = \epsilon \beta x^2 \tag{4.11}$$

Here, ϵ is the air-water density ratio, $\rho_a(0)/\rho_w(0)$ and β the so-called Miles parameter, which is defined by

$$\beta = \frac{\beta_m}{\kappa c} \mu ln^4(\mu), \quad \mu \leq 1 \tag{4.12}$$

where β_m is a constant and μ defined by

$$\mu = \left(\frac{u_*}{\kappa c}\right)^2 \Omega_m exp\left(\frac{\kappa}{x}\right) \tag{4.13}$$

The input source term of the WAM-model is given by

$$S_{in} = \gamma N \tag{4.14}$$

where N is the action density spectrum.

Eq. 4.10-4.14 are dependent on the stress of air flow over the surface which again depends on the sea state. Janssen (1991) considered the momentum balance of air and found the kinematic stress to be expressed as

$$\tau = u_*^2 = \left(\kappa \frac{U(z_{obs})}{ln\left(z_{obs}/z_0\right)} \right)^2 \tag{4.15}$$

where u_* is the friction velocity, z_{obs} is the mean height above the waves and the roughness length is defined by

$$z_0 = \frac{\hat{\alpha}\tau}{g\sqrt{1-y}}, \quad y = \frac{\tau_w}{\tau} \tag{4.16}$$

τ_w is the stress induced by the surface waves and is defined by

$$\tau_w = \epsilon^{-1} g \int d\omega d\theta \, \gamma N \mathbf{k} \tag{4.17}$$

Whenever the wave induced stress becomes of the order of the total stress the roughness length gets enhanced and the momentum transfer from air to sea is more efficient.

Finally we are left with two unknown constants, β_m and $\hat{\alpha}$, which have both been estimated by comparing observational and numerical results to find the best fit. They are found to be $\beta_m = 1.2$ and $\hat{\alpha} = 0.01$.

The dissipation term of the WAM-model has a less complicated form than the input and nonlinear term. This is basically because dissipation by whitecapping is a highly nonlinear term not well understood. The term is given by

$$S_{dis} = -C_{dis} \, \bar{\omega} \left(\bar{k}^2 \, m_0\right)^2 \left[\frac{(1-\delta)k}{\bar{k}} + \delta \left(\frac{k}{\bar{k}} \right)^2 \right] N \tag{4.18}$$

Here $\bar{\omega}$ and $\bar{k}$ are the mean angular frequency and mean wave number respectively. In practice, the constants are set to $C_{dis} = 4.5$ and $\delta = 0.5$. It should also be mentioned that the dissipation term by bottom friction is expressed as

$$S_{bot} = -C_{bot} \frac{k}{sinh(2kh)} N \tag{4.19}$$

where $C_{bot} = 0.038/g$ and h is the depth.

The Boltzmann-type integral is a highly time consuming expression to calculate exactly. In the WAM-model the integral is parameterized using the DIA(discrete interaction approximation) (Hasselmann and Hasselmann (1985); Hasselmann et al. (1985)). Without going to much into detail, this approach applies the same integration method used to integrate the exact source term, but instead of integrating over the five-dimensional interaction phase space, the integration is taken over a two dimensional continuum and two discrete interactions. The reader is referred to Hasselmann and Hasselmann (1985) for an in depth presentation.

4.3.2 Numerical schemes

Fig. 4.2 illustrates the most commonly used frequency resolution of the WAM-model, with a minimum frequency $f_{min} = 0.042$ and a maximum frequency $f_{max} = 0.42$. In between, the discrete frequency centers are represented by $f_i = (1.1)^{i-1} f_{min}$. This offers a total of 25 frequency bands, $i = 25$, where each individual interval is defined by $\Delta f = 0.1f$. The frequency bands are represented in 24 directional sectors, offering a 15° resolution.

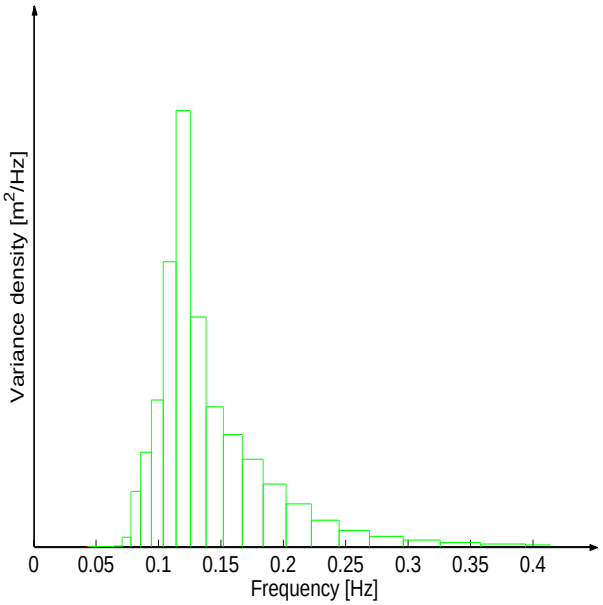

Figure 4.2: *Frequency resolution used in the WAM-model*

In the WAM-model, the wave spectrum distinguishes between a prognostic part, f_{min} to f_{hf}, and a diagnostic part. The diagnostic part is represented by an predetermined f^{-5} tail and has the same directional distribution as the last frequency band of the prognostic region. The tail is expressed given by;

$$E(f,\theta) = E(f_{hf},\theta)\left(\frac{\bar{f}}{f_{hf}}\right)^{-5} \quad \text{for} \quad f > f_{hf} \tag{4.20}$$

, where the high-frequency limit is defined by

$$f_{hf} = \min\{f_{max}, \max(2.5\bar{f}, 4f_{PM})\} \tag{4.21}$$

With the high frequency limit the spectrum is scaled for young waves by the mean frequency $\bar{f}$ and for more developed wind-seas by the Pierson-Moskowitz-frequency $f_{PM} = 4.57 \cdot 10^{-3}$ (Massel 1996). The diagnostic tail is mainly needed to compute the nonlinear transfer and the dissipation of the prognostic region. While the diagnostic part of the wave spectrum is predetermined, the prognostic part has to be calculated numerically by solving the energy balance equation.

Source functions

The WAM-model uses an implicit second order scheme to simulate the evolution of the source terms. The advantage of this scheme is found in its ability to use an integration time-step that is greater than the dynamical adjustment time of the highest frequencies still treated prognostically in the model.

The implicit second order, centered difference equation is expressed by

$$E_{n+1} = E_n + \frac{\Delta t}{2}(S_{n+1} + S_n) \tag{4.22}$$

where Δt is the time step and n refers to the time level. If the source functions had been linear eq. 4.22 could have been solved directly. Since this is not the case a Taylor expansion is introduced

$$S_{n+1} = S_n + \frac{\partial S_n}{\partial E}\Delta E + ... \tag{4.23}$$

S_{n+1} is then expressed numerically by a discrete matrix, M_n, and divided into a diagonal,Λ_n, and non-diagonal matrix, N_n

$$\frac{\partial S_n}{\partial E} = M_n = \Lambda_n + N_n \tag{4.24}$$

By substituting eq. 4.23-4.24 into 4.22, and considering that the source terms may depend on the friction velocity u^*, it can be showed that the change of the wave spectrum, $\Delta E = E_{n+1} - E_n$, is given by

$$\Delta E = \frac{\Delta t}{2}\left(S_n(u_*^n) + S_n(u_*^{n+1})\right)\left[1 - \frac{\Delta t}{2}\Lambda_n(u_*^{n+1})\right]^{-1} \tag{4.25}$$

Computations show that the non-diagonal contribution is insignificant and is therefore not taken into account.

Advection and refraction

The advection term of the energy balance equation is expressed in flux form and its evolution is solved using a first order up-winding scheme. This scheme is chosen because it is easy to implement, requiring less computer time and memory. And, the results have been satisfactory.

Here, only an one dimensional case is illustrated, simply because the analogy to more dimensions is straight forward. Lets consider the advection equation given by;

$$\frac{\partial}{\partial t}E = -\frac{\partial}{\partial x}\Phi, \tag{4.26}$$

where $\Phi = c_g E$, then the rate of change of the spectrum in the jth grid point is given by;

$$\Delta E_j = -\frac{\Delta t}{\Delta x}(\Phi_{j+1/2} - \Phi_{j-1/2}). \tag{4.27}$$

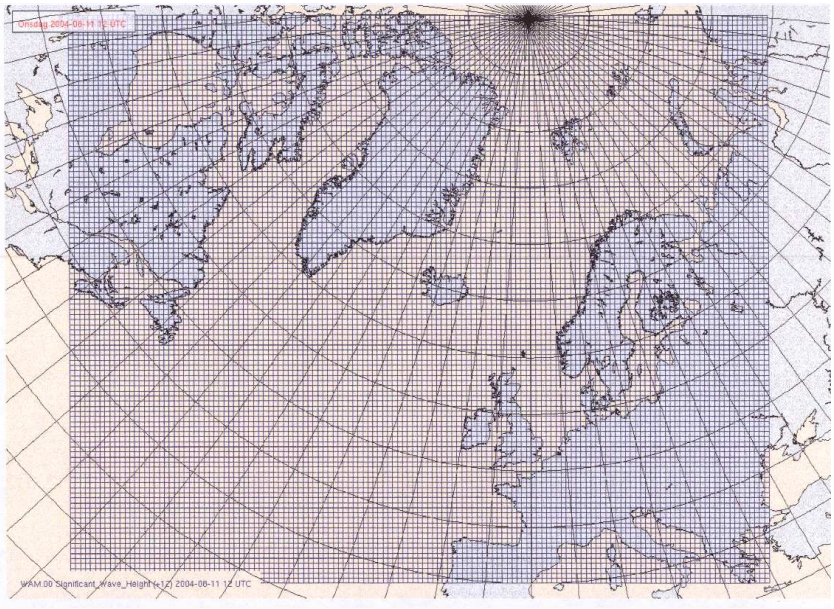

Figure 4.3: *The area of which the WAM-model is run operationally at met.no. The grid spacing is given at 50km.*

Here the Δx is the grid spacing and;

$$\Phi_{j\pm1/2} = \frac{1}{2}[v_j + |v_j|]E_j + \frac{1}{2}[vj - |v_j|]E_{j+1} \tag{4.28}$$

where $v_j = 0.5(c_{g,j} + c_{g,j\pm1})$ is the mean group velocity. This concludes the numerical schemes used in the WAM-model.

4.3.3 The WAM-model run at met.no

Set-up/Grid and boundary conditions

At the Meteorological Institute of Bergen(met.no) the WAM-model is run operationally. The modelled area, see fig. 4.3, has a grid spacing of $\Delta x = 50$km and closed boundaries set to zero. Energy generated outside the boundaries, advected across, are not simulated.

Input/Output

The WAM-model is, as mentioned, only dependent of 10m winds covering the modelled area. At met.no these wind fields are obtained from the atmospheric model HIRLAM-20, introduced in the next section, forcing the wave model every three hours. Integration time step is $\Delta t = 15$min. Wind fields for each time step are calculated using linear interpolation in between every three hours the HIRLAM-20 simulates new wind fields.